Temperature Dependence of Hysteresis and the Pore Size Distributions of Two Mesoporous Adsorbents

William D. Machin

Department of Chemistry, Memorial University of Newfoundland, St. John's, Newfoundland, Canada A1B 3X7

Received June 2, 1993. In Final Form: December 2, 1993[⊛]

Isotherms at integer temperatures for xenon (210–260 K) and argon (120–142 K) on a mesoporous silica gel show that with increasing temperature (T) hysteresis decreases, vanishing at a capillary critical temperature (T_{cc}), a temperature lower than the bulk critical temperature (T_c). The desorption branches of all isotherms below T_{cc} exhibit a nearly vertical step which corresponds to the first-order transition, capillary liquid to capillary gas. Using current theories of fluids in pores, a new method for the estimation of pore size distribution (PSD) is developed. The analysis requires a large number of isotherms at temperatures approaching T_{cc}, which, for many mesoporous adsorbents, involves operating at pressures up to *ca.* 3300 kPa. Both adsorptives give essentially the same PSD. This method of PSD analysis is also applied to published isotherms for xenon and carbon dioxide on Vycor porous glass. A less exact PSD analysis, requiring only a single isotherm at or near the normal boiling point of the adsorptive, is also developed.

As pressure (P) increases, adsorption in mesoporous adsorbents is traditionally assumed to progress from monolayer to multilayers until the entire pore structure fills with capillary condensed liquid. Conversely, as P decreases, desorption results in the removal of liquid from pores by capillary evaporation. Hysteresis is presumed to arise when capillary evaporation occurs across a liquid–vapor interface different from that present during adsorption. Methods for pore size analysis based on this model are now well established.[1] This model, however, fails to accommodate the experimentally observed diminution and disappearance of the hysteresis loop at some temperature less than T_c, the bulk critical temperature.[2] Furthermore, within the upper plateau region characteristic of type IV isotherms with H2 hysteresis,[3] the adsorbate is present as capillary liquid,[4,5] and while this agrees with the traditional model of fluids in capillaries, we have found that on the adsorption branch the adsorbate is present as capillary gas not as capillary liquid.[5] This implies that the steeply descending segment in the desorption branch of the hysteresis loop corresponds to a first-order transition, capillary liquid to capillary gas. These observations cannot be explained by the traditional model of hysteresis, but they are readily accommodated by current theories of adsorption in small pores.[6,7] In this work we present a method for pore size distribution analysis based on these theories and examine some of the inferences arising from this model.

Experimental Section

Xenon (Matheson, research purity, 99.995%) and argon (Matheson, prepurified, 99.998%) were used as supplied. The preparation and properties of the adsorbent, mesoporous silica gel SG3, are described elsewhere.[8] The adsorption apparatus is similar to that described earlier,[5,9] but is constructed of stainless steel components rated for pressures to 1000 psi (6890 kPa). Pressures to *ca.* 3300 kPa are measured with a MKS Baratron pressure sensor (type 590 HA-25000) to a precision of *ca.* 0.05%. Pressures were verified periodically by comparison of measured saturation vapor pressures against reference values.[10] Isotherms for oxygen, *n*-butane, and tetrachloromethane were determined gravimetrically or with a low-pressure volumetric apparatus. These adsorptives had a purity of at least 99.9 mol %.

Results and Discussion

Complete isotherms for xenon are measured at integer temperatures from 210 to 260 K and for argon from 120 to 142 K. All isotherms are type IV with H2 hysteresis. Examples of these are shown in Figure 1. Although isotherms for xenon and argon appear similar, the total pore volume available to argon is greater by *ca.* 0.022 cm^3 g^{-1}. Similar isotherms have been reported by Burgess[11] and Nuttal[12] for xenon and carbon dioxide adsorbed on porous Vycor glass. These results also demonstrate that as $T \rightarrow T_c$ the extent of hysteresis decreases and eventually vanishes at a capillary critical temperature, T_{cc}, where $T_{cc} < T_c$. Type II isotherms with H3 hysteresis[3] have been reported by Michalski *et al.*[13] for the adsorption of sulfur hexafluoride on a mesoporous graphitic carbon described as having "an ill-defined, wide distribution of pore sizes". Nevertheless, the extent of hysteresis decreases as $T \rightarrow T_c$, and its presence at the highest temperature studied, $T/T_c = 0.985$, is ascribed to condensation in very wide pores. More recently, using controlled pore glass as an adsorbent, Findenegg *et al.*[14] have shown that hysteresis

[⊛] Abstract published in *Advance ACS Abstracts*, February 15, 1994.

(1) Gregg, S. J.; Sing, K. S. W. *Adsorption, Surface Area and Porosity*, 2nd ed.; Academic Press: New York, 1982; Chapter 3.
(2) Everett, D. H. In *Studies in Surface Science and Catalysis, Vol. 39, Characterization of Porous Solids*; Unger, K. K., Rouquerol, J., Sing, K. S. W., Kral, H.; Eds.; Elsevier: Amsterdam, 1988; p 1.
(3) Sing, K. S. W.; Everett, D. H.; Haul, R. A. W.; Moscou, L.; Pierotti, R. A.; Rouquerol, J.; Siemieniewska, T. *Pure Appl. Chem.* **1985**, *57*, 603.
(4) Machin, W. D.; Golding, P. D. *J. Chem. Soc., Faraday Trans.* **1990**, *86*, 171.
(5) Machin, W. D. *J. Chem. Soc., Faraday Trans.* **1992**, *88*, 729.
(6) Evans, R.; Marconi, U. M. B.; Tarazona, P. *J. Chem. Soc., Faraday Trans. 2*, **1986**, *82*, 1763 and references therein.
(7) Ball, P. C.; Evans, R. *Langmuir* **1989**, *5*, 714 and references therein.
(8) Machin, W. D.; Golding, P. D. *Langmuir* **1989**, *5*, 608.
(9) Machin, W. D.; Golding, P. D. *J. Chem. Soc., Faraday Trans. 1* **1987**, *83*, 1203.
(10) Younglove, B. A. *J. Phys. Chem. Ref. Data* **1982**, *11*, Suppl. No. 1.
(11) Burgess, C. G. V. Ph.D. Thesis, University of Bristol, 1971. See also Burgess, C. G. V.; Everett, D. H.; Nuttal, S. *Pure Appl. Chem.* **1989**, *61*, 1845.
(12) Nuttal, S. Ph.D. Thesis, University of Bristol, 1974. See also ref 7 and Burgess, C. G. V.; Everett, D. H.; Nuttal, S. *Langmuir* **1990**, *6*, 1734.
(13) Michalski, T.; Benini, A.; Findenegg, G. H. *Langmuir* **1991**, *7*, 185.
(14) Findenegg, G. H.; Gross, S.; Michalski, Th.; Thommes, M. IUPAC Symposium on the Characterization of Porous Solids, May 1993; Abstract 9.

0743-7463/94/2410-1235$04.50/0

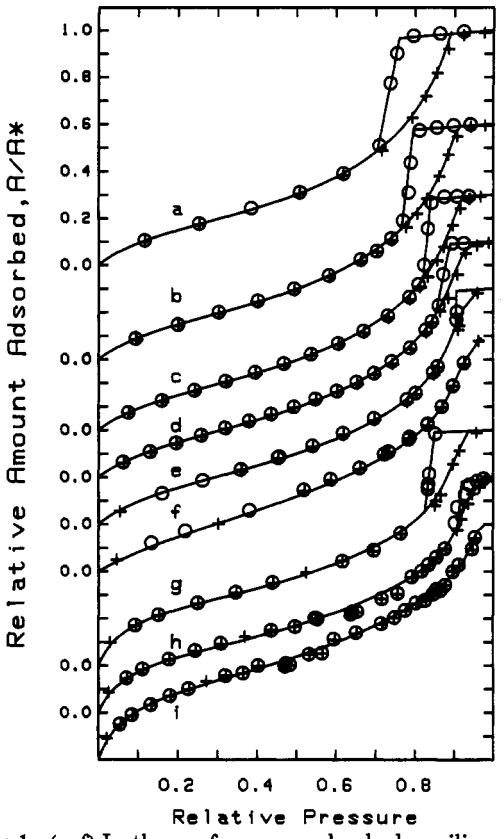

Figure 1. (a–f) Isotherms for xenon adsorbed on silica gel SG3 at 210, 220, 230, 240, 250, and 260 K, respectively. (g–i) Isotherms for argon adsorbed on SG3 at 120, 130, and 140 K, respectively. Note the diminution in the size of the hysteresis loop as temperature increases. Isotherms are offset for clarity.

due to pore condensation disappears at $T_{cc} < T_c$ and that this critical point shift is inversely proportional to the pore width, *i.e.*, $1 - T_{cc}/T_c \propto 1/R_P$. This observation is in accord with current theoretical predictions for the behavior of fluids in small pores. Evans *et al.*[6,15] have derived, for a cylindrical pore of radius R_P, the relation

$$1 - T_{cc}/T_c \approx d/R_P \tag{1}$$

where d is taken to be the molecular diameter of the adsorbate. A similar equation is obtained for slit-shaped pores. This equation is only approximate, and the authors suggest that it should be most appropriate within the following limits: $2 \leq R_P/d \leq 20$ and $T_{cc} < 0.95\ T_c$. It is clear from eq 1 that for $T > T_{cc}$ adsorption is reversible and for $T < T_{cc}$ it is not. Consequently, for a given T_{cc}, pores with radii greater than R_P will exhibit hysteresis whereas those with smaller radii will not.

For bulk fluids at $T < T_c$, the difference between the liquid- and gas-phase densities, $\Delta\rho$, depends on temperature according to[16]

$$\Delta\rho \propto [1 - T/T_c]^{\beta} \tag{2}$$

where $\beta \simeq 1/3$. In pores the density of capillary liquids is comparable to that of the bulk liquid, but the average density of the capillary gas is usually much larger than that of the bulk gas. The coexistence curve for capillary fluids is therefore shifted to a lower critical temperature and to higher densities on the gas branch. Examples have been presented by Burgess *et al.*[17] and Findenegg *et al.*[14] The former conclude that the top of the step segment in the desorption branch of the hysteresis loop corresponds to capillary liquid filling the pores. As $T \rightarrow T_{cc}$ the average density of the capillary gas phase at the lower closure point of the hysteresis loop approaches that of the capillary liquid, and the densities become equal at T_{cc}. Michalski *et al.*[13] have shown for SF_6 adsorbed on a mesoporous graphitic carbon that at $T < 0.95T_c$ the temperature dependence of $\Delta\rho$ obeys eq 2. We have reported similar behavior for xenon adsorbed on silica gel.[4] It therefore seems reasonable to suggest for capillary fluids

$$\Delta\rho \propto [1 - T/T_{cc}]^{\beta};\ \beta = 1/3 \tag{2a}$$

However it should be noted for wide pore distributions that, at a given relative fugacity, the average density of capillary gas in small pores will be greater than that in larger pores. Consequently, eq 2 may be less exact for such pore systems.

Implicit in the application of eqs 1 and 2 to pore size analysis is the assumption that irregular, interconnected real pore structures can be represented by an assembly of independent cylindrical pores. The validity or at least the utility of such nominal or apparent pore size distributions (PSD) based on this model should therefore be tested against the following criteria: (i) the PSD should be independent of the adsorbate and (ii) the adsorbent surface area derived from the PSD should be equal to the Brunauer–Emmett–Teller (BET) surface area.

Since pore volume, V_p, is fixed, the densities of the capillary phases are A_d/V_p and A_a/V_p, where A_d and A_a are the amounts adsorbed at the top and bottom of the step, respectively. Hence,

$$\Delta\rho = (A_d/V_p) - (A_a/V_p) = k[1 - T/T_{cc}]^{1/3} \tag{3}$$

As $T \rightarrow 0$, A_d remains $\simeq A^*$, the amount adsorbed at the saturation pressure, but $A_a \rightarrow 0$; hence, $k = A^*/V_p$, giving

$$\Delta A = (A_d/A^*) - (A_a/A^*) = [1 - T/T_{cc}]^{1/3} \tag{4}$$

where $\Delta A = V_p\Delta\rho/A^*$. Then for a single pore, or a group of pores of equal radii, ΔA will increase as T decreases below T_{cc}.

The same phenomenon will be observed for an assembly of pores of different radii, as observed in this and other work.[4,11,12] If each pore acts independently with respect to the capillary phase transition, a pore size distribution (PSD) may be derived from a set of isotherms such as those in Figure 1. The maximum pore radius, R_o, is readily calculated (eq 1) from the observed capillary critical temperature, T_o, and since the volume in pores of $R > R_o$ must be zero, then $V_o = 0$. At the next lowest temperature, T_1, we obtain from eq 4

$$\Delta A_1 = K_1[1 - T_1/T_0]^{1/3} \tag{5}$$

where K_1 is the volume fraction in pores of radii R such that $R_1 < R < R_o$, where $R_1 = d/[1 - T_1/T_c]$. Pores with radii less than R_1 do not contribute to ΔA_1, since their capillary critical temperature is less than T_1. At the next lower temperature, T_2,

$$\Delta A_2 = K_1[1 - T_2/T_0]^{1/3} + K_2[1 - T_2/T_1]^{1/3} \tag{6}$$

where the first term is the contribution to ΔA_2 from the

(15) Evans, R.; Marconi, U. M. B.; Tarazona, P. *J. Chem. Phys.* **1986**, *84*, 2376.
(16) Fisher, M. E. *J. Math. Phys.* **1964**, *5*, 944.
(17) Burgess, C. G. V.; Everett, D. H.; Nuttal, S. *Pure Appl. Chem.* **1989**, *61*, 1845.

Table 1. Pore Size Distribution Analysis for Silica Gel SG3

n^a	T^b/K	ΔA^b	$\sum^c$	$R_n{}^d$/nm	$V_R{}^e$/ (cm^3 g^{-1})	$S_R{}^f$/ (m^2 g^{-1})
			I. From Argon Isotherms			
0	139	0.000	0.0000	4.51	0.0000	0
1	138	0.014	0.0143	4.15	0.0235	11
2	137	0.040	0.0434	3.85	0.0651	32
3	136	0.066	0.0749	3.59	0.1016	51
4	135	0.090	0.1024	3.36	0.1260	65
5	134	0.115	0.1281	3.16	0.1461	78
6	133	0.134	0.1480	2.98	0.1559	84
7	132	0.159	0.1721	2.82	0.1742	97
8	131	0.181	0.1952	2.68	0.1894	108
9	130	0.200	0.2138	2.55	0.1967	113
10	129	0.219	0.2320	2.43	0.2050	120
11	128	0.235	0.2482	2.32	0.2105	125
12	127	0.249	0.2615	2.23	0.2125	126
13	126	0.264	0.2754	2.14	0.2171	131
14	125	0.278	0.2887	2.05	0.2210	134
15	124	0.294	0.3040	1.98	0.2287	142
16	123	0.308	0.3187	1.91	0.2348	148
17	122	0.320	0.3305	1.84	0.2366	150
18	121	0.330	0.3405	1.78	0.2365	150
19	120	0.342	0.3513	1.72	0.2391	153
			II. From Selected Xenon Isotherms			
0	262	0.000	0.0000	4.52	0.0000	0
1	257	0.063	0.0632	3.83	0.0698	33
4	254	0.097	0.1050	3.51	0.1101	55
8	250	0.155	0.1641	3.16	0.1676	90
12	246	0.218	0.2283	2.87	0.2108	118
17	241	0.274	0.2826	2.57	0.2232	127
23	235	0.310	0.3150	2.29	0.2172	122
30	228	0.370	0.3760	2.03	0.2420	144
37	221	0.419	0.4240	1.83	0.2547	157
45	213	0.470	0.4749	1.64	0.2705	175
48	210	0.487	0.4710	1.57	0.2732	178

[a] Values of n used in eqs 7–11; i = 1, 2, 3, ..., n. [b] Experimental data, T_n and ΔA_n, taken from the isotherms (see Figure 1). [c] $\sum$ is $\sum_{i=1}^{n} K_i[1 - T_n/T_{i-1}]^{1/3}$ calculated from eq 7. Ideally, values in this column should be the same as ΔA. [d] The minimum pore size which contributes to hysteresis at temperature T, calculated from eq 8. [e] Cumulative volume in pores of radii greater than R_n, calculated from eq 10. [f] Cumulative surface area in pores having radii greater than R_n, calculated from eq 11.

first group of pores (K_1, R_1) at T_2 and the second term is the contribution from those pores of radii R such that $R_2 < R < R_1$ where, as before, $R_2 = d/[1 - T_2/T_c]$. At T_2 the pore volume contributing to hysteresis is proportional to $K_1 + K_2$. In general, for T decreasing from T_1 to T_n,

$$\Delta A_n = \sum_{i=1}^{n} K_i[1 - T_n/T_{i-1}]^{1/3} \tag{7}$$

and

$$R_n = d/[1 - T_n/T_c] \tag{8}$$

For each isotherm, these equations yield values of R_n, and K_n, and V_n is obtained from

$$V_n = K_n V_p \tag{9}$$

where V_n is the volume in pores of radii R where $R_n < R < R_{n-1}$. Hence, the total volume in pores of radii $R > R_n$ is

$$V_R = \sum_{i=1}^{n} V_i \tag{10}$$

and the surface area, S_R, in these pores is given by

$$S_R = \sum_{i=1}^{n} S_i = \sum_{i=1}^{n} 4V_i/[R_i + R_{i-1}] \tag{11}$$

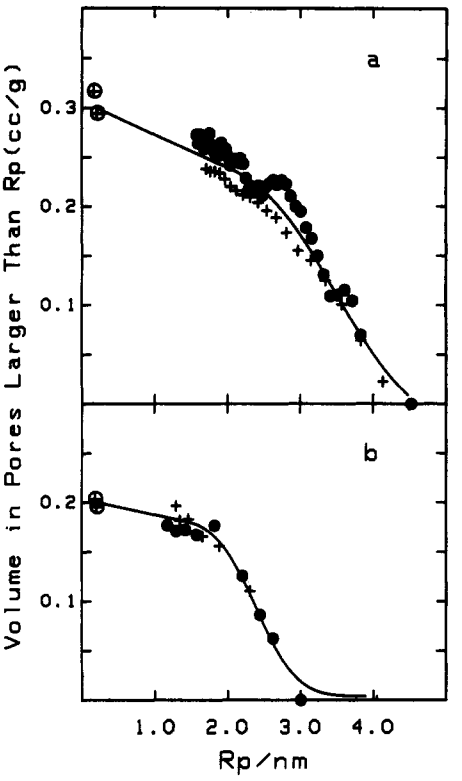

Figure 2. (a) Cumulative pore size distribution for xenon (●) and argon (+) on silica gel SG3. (b) Cumulative pore size distribution for xenon (●) and carbon dioxide (+) on Vycor porous glass. Points marked ⊕ correspond to a total pore volume estimated from the amount adsorbed at the saturation pressure with the minimum pore radius taken as half the diameter of the adsorptive.

In principle, an appropriate series of isotherms will yield the pore size distribution, pore volume, and surface area of an adsorbent. In practice, however, there is a lower limit with respect to pore size, since at low temperatures other phenomena such as prewetting and partial wetting[5] may influence ΔA or the capillary liquid may freeze. When part of the pore volume is excluded from the analysis, V_R will be less than the total pore volume and S_R will be less than the total surface area.

A summary of calculations for argon and xenon adsorbed on SG3 is given in Table 1, and the PSD is shown in Figure 2. Within the limitations of this analysis, both sets of isotherms are described by a single pore distribution. Earlier work has shown that pores of radii comparable to the diameter of xenon are not present in this adsorbent.[8] Therefore, from the data in Table 1 and Figure 2, there is a small pore volume (*ca.* 0.04 cm^3 g^{-1}) within pores of radius less than 1.5 nm but greater than 0.86 nm (twice the diameter of xenon). The surface area in these pores is *ca.* 68 m^2 g^{-1}, raising the total calculated pore area to *ca.* 220–230 m^2 g^{-1} (see Table 1), a value in excellent agreement with the BET (N_2) surface area of 223 m^2 g^{-1}. This agreement suggests that this method of pore size analysis, when taken in conjunction with the total pore volume, enables the estimation of the complete pore size distribution for this mesoporous silica gel.

We obtain the same conclusion when this analysis is applied to the adsorption of xenon and carbon dioxide on porous Vycor glass.[11,12] Calculations are summarized in Table 2, and the PSD is shown in Figure 2. Clearly, both sets of isotherms are described by a single pore size distribution which extrapolates smoothly to the total pore volumes for these adsorptives. The volume in pores with

Table 2. Pore Size Distribution Analysis for Vycor Porous Glass[a]

n	T/K	ΔA	Σ	R_n/nm	V_R/ (cm^3 g^{-1})	S_R/ (m^2 g^{-1})
			I. From Carbon Dioxide Isotherms[b]			
0	275	0.000	0.0000	4.06	0.0000	0
1	252.98	0.235	0.2350	2.32	0.1112	70
2	241.78	0.314	0.3485	1.90	0.1568	113
3	233.26	0.364	0.4017	1.67	0.1664	124
4	224.22	0.431	0.4676	1.48	0.1841	146
5	217.45	0.465	0.4944	1.37	0.1823	144
			II. From Xenon Isotherms[c]			
0	248	0.000	0.0000	3.01	0.0000	0
1	242.89	0.093	0.0928	2.62	0.0625	44
2	238.35	0.123	0.1379	2.44	0.0864	63
3	232.84	0.195	0.2234	2.21	0.1256	97
4	221.14	0.319	0.3851	1.83	0.1766	148
5	210.36	0.367	0.4313	1.58	0.1670	136
6	201.87	0.440	0.4761	1.43	0.1722	143
7	193.18	0.474	0.5080	1.30	0.1709	141
8	183.45	0.519	0.5517	1.18	0.1768	151

[a] See footnotes to Table 1. [b] Data taken from ref 11. [c] Data taken from ref 12.

radii less than 1.3 nm is *ca.* 0.02 cm^3 g^{-1} (Table 2), and the area in these pores, assuming an average radius of 1.0 nm, is 40 m^2 g^{-1}. This gives a total surface area of 180–185 m^2 g^{-1}, a value in excellent agreement with BET (N_2) areas reported by Burgess[11] (180.6 m^2 g^{-1}) and Nuttal[12] (187.1 m^2 g^{-1}).

The adsorbents considered here, silica gel SG3 and porous Vycor glass, are rigid materials with well-defined pore volumes and negligible external surface area, and which typically give type IV isotherms with H2 hysteresis for a variety of adsorptives. Some examples have been published,[5,8,11,12,18] and others are shown in Figure 3. The steep segment in the desorption branch characteristic of these isotherms is often ascribed to network, or pore-blocking, effects in a pore structure consisting of cavities connected by smaller necks.[19] If network effects are important, removal of capillary condensed liquid from a cavity may be delayed until at least one connecting neck is emptied by irreversible capillary evaporation. In contrast, the model presented here excludes the basis of that explanation, since adsorption or desorption in necks will be reversible at temperatures lower than that required for reversibility in larger cavities. Furthermore, this steep segment persists even at temperatures close to the capillary critical temperature (see Figure 1), where the fraction of pores that exhibit hysteresis is so small that effective pore-blocking must be insignificant. This phenomenon is, however, consistent with a model based on a first-order phase change in the capillary fluid. We therefore conclude that network effects are relatively unimportant and that pore size distributions derived from this method reflect the cavity size distribtion of those cavities in which an irreversible, first-order, capillary phase transition can occur. A similar conclusion is reported by de Keizer *et al.*[20] for SF_6 adsorbed in controlled pore glass.

Apart from the constraints imposed by the limitations of eqs 1 and 2, the largest experimental error arises in the estimation of the average density of the capillary gas phase at the phase transition. This quantity A_a/A^* is determined at the intersection of the steep desorption branch with the adsorption branch. The angle of intersection may be small (see Figure 1), resulting in a relatively large uncertainty in the density estimated for the capillary gas. To minimize this problem, we have resorted to a smoothing procedure, illustrated in Figure 5, where a line is drawn through the set of lower closure points. The various ΔA_n are determined as differences between the line and the density of the capillary liquid phase, A_d/A^*, at each temperature. Finally, it should also be noted that experimental error in the amounts adsorbed, A_a and A_d, increases significantly at high gas-phase densities, and may be as large as 1% for isotherms near T_{cc}. While all of the above determine the accuracy of the analysis, the major disadvantage of this method is the time required to amass sufficient data to support the analysis. Some of our systems required more than six months of almost continuous data collection. This problem encouraged us to develop a more convenient method of analysis.

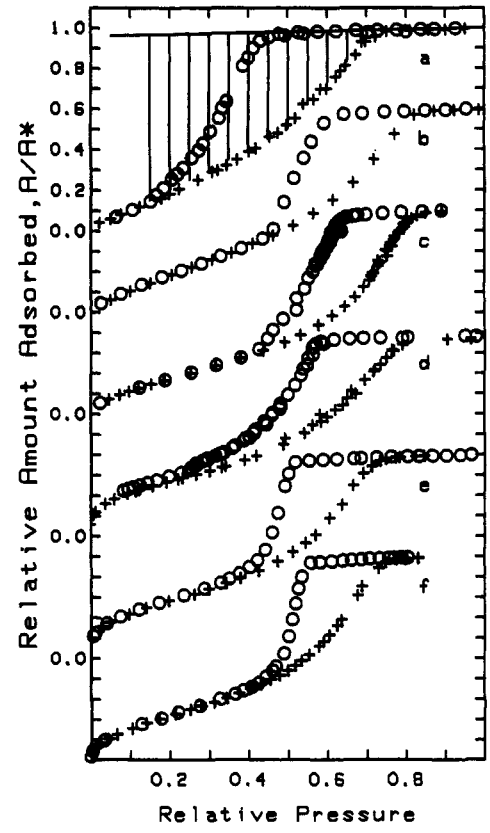

Figure 3. Isotherms for various adsorptives on silica gel SG3 and Vycor porous glass (VPG): (a) tetrachloromethane on SG3 at 283.3 K, (b) *n*-butane on SG3 at 273.4 K, (c) xenon on SG3 at 169 K, (d) oxygen on SG3 at 77.5 K, (e) krypton on VPG at 117.41 K (from ref 18), (f) xenon on VPG at 168.25 K (from ref 18). The isotherm construction used to determine ΔX (eq 12) is illustrated in (a).

When plotted as relative amount adsorbed, A/A^*, against the relative pressure, P/P^*, or relative fugacity, f/f^*, the position of the adsorption branch changes only slowly with temperature and the position of the upper plateau is nearly constant. A series of "isotherms", similar in appearance to those in Figure 1, can be constructed by connecting the adsorption branch of the isotherm to the capillary liquid branch at various relative pressures. The capillary liquid branch may be extrapolated, if necessary, to low relative pressures. This construction is illustrated in Figure 3. The length, ΔX, of each vertical segment corresponds to ΔA in eq 4, *i.e.*

$$\Delta X = (A_d/A^*) - (A_a/A^*) = [1 - T/T_{cc}]^{1/3} \quad (12)$$

(18) Brown, A. J. Ph.D. Thesis, University of Bristol, 1963. See also ref 19 and Everett, D. H. In *The Solid-Gas Interface*; Flood, E. A., Ed.; Marcel Dekker: New York, 1967; Vol. 2, Chapter 36.

(19) Mason, G. *Proc. R. Soc. London* **1988**, *A415*, 453.

(20) de Keizer, A.; Michalski, T.; Findenegg, G. H. *Pure Appl. Chem.* **1991**, *63*, 1495.

(21) Ben-Amotz, D.; Herschback, D. R. *J. Phys. Chem.* **1990**, *94*, 1038.

Table 3. Comparison of Calculated and Experimental Hysteresis Closure Points

adsorbent	adsorptive	T/K	lower closure calcd	lower closure obsd	upper closure calcd	upper closure obsd	d^a/nm	V_p/(cm^3 g^{-1})
SG3	O_2	77.5	0.140	0.22	0.837	0.80	3.46	0.312
	Xe	169.0	0.335	0.43	0.835	0.84	4.33	0.270
	C_4H_{10}	273.4	0.460	0.46	0.787	0.82	5.86	0.286
	CCl_4	266.1	0.110	0.11	0.696	0.69	6.04	0.278
	CCl_4	283.3	0.155	0.16	0.709	0.72	6.04	0.278
VPG[b]	Kr	117.41	0.276	0.34	0.756	0.74	3.87	0.189
	Xe	168.25	0.330	0.43	0.740	0.76	4.33	0.181

[a] Molecular diameters (d) are calculated using the method in ref 21. [b] Data for Vycor porous glass (VPG) are taken from ref 18.

Table 4. Pore Size Distribution Calculation for Silica Gel SG3 from a Single Isotherm, Xenon at 169 K[a]

n	P/P^*[b]	ΔX[b]	T[c]/K	Σ	R_n/nm	V_R/(cm^3 g^{-1})	S_R/(m^2 g^{-1})
0	0.840	0.000	262.6	0.0000	4.63	0.0000	0
1	0.820	0.020	259.6	0.0200	4.16	0.0238	11
2	0.800	0.040	256.6	0.0451	3.79	0.0477	23
3	0.780	0.090	253.5	0.0991	3.46	0.1005	52
4	0.760	0.140	250.1	0.1597	3.17	0.1471	80
5	0.740	0.210	245.7	0.2415	2.85	0.1991	115
6	0.720	0.260	240.9	0.2987	2.57	0.2176	128
7	0.700	0.320	234.5	0.3641	2.27	0.2369	144
8	0.680	0.370	227.6	0.4129	2.02	0.2421	149
9	0.660	0.410	220.7	0.4461	1.82	0.2396	147
10	0.640	0.440	214.5	0.4676	1.67	0.2341	140
11	0.620	0.460	209.3	0.4793	1.56	0.2271	132

[a] See footnotes to Table 1. [b] Experimental data, P/P^* and ΔX, taken from the isotherm (see Figure 3). [c] T is T_{xc} calculated using eqs 13–16.

and the corresponding relative pressure can be related to an appropriate temperature, T_x, as follows.

At the upper closure point of the hysteresis loop where $\Delta X = 0$, $T = T_{cc}$. Hence (eq 1)

$$T = T_c[(R_p - d)/R_p] \tag{13}$$

In the presence of an adsorbed monolayer film the Kelvin equation for a hemispherical meniscus in a cylindrical pore is

$$RT \ln(P/P^*) = -2\gamma V/(R_p - d) \tag{14}$$

Then from eq 13

$$(R_p - d)^2/R_p = -2\gamma V/[RT_c \ln(P/P^*)] \tag{15}$$

where P/P^* is the relative pressure at the upper closure point of the hysteresis loop and R_p is the radius of the largest pore. V and γ are the molar volume and surface tension, respectively, of the adsorbate. This equation, with $R_p = 4.51$ nm for SG3 and 3.00 nm for porous Vycor glass, has been used to calculate the relative pressures at the upper closure point for the isotherms shown in Figure 3. It is clear from the results summarized in Table 3 that eq 15 provides a reasonable estimate of the position of the upper closure point of the hysteresis loop.

For our present purposes, however, we use eq 15 to calculate R_p at selected relative pressures. The maximum pore size, R_o, is readily calculated for $\Delta X = 0$, and the corresponding capillary critical temperature, T_o, is calculated from eq 13. At other relative pressures, T_x values calculated for xenon on silica gel SG3 at 169 K and on porous Vycor glass at 168.24 K diverge from experimental T_n values as ΔX increases. We have therefore applied an empirical factor to adjust calculated T_x values, namely

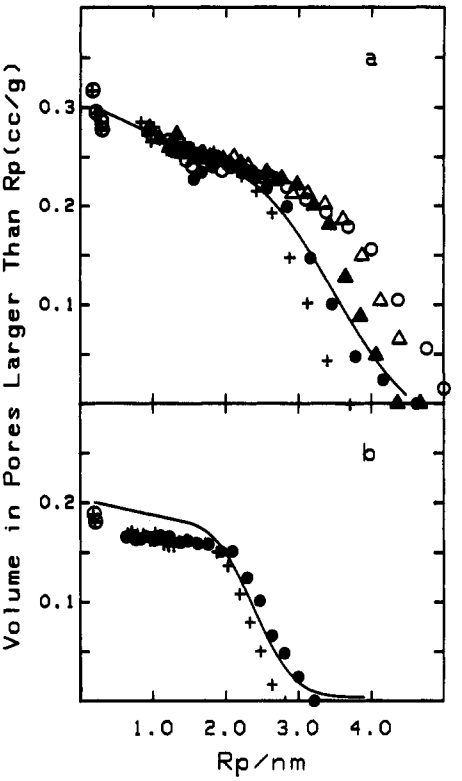

Figure 4. Cumulative pore size distributions obtained from single isotherms: (a) silica gel SG3, oxygen at 77.5 K (+), xenon at 169 K (●), tetrachloromethane at 266.1 K (▲) and 283.3 K (△), n-butane at 273.4 K (○); (b) Vycor porous glass, krypton at 117.41 K (+), xenon at 168.25 K (●). The solid lines in (a) and (b) correspond to the solid lines in parts a and b of Figure 2. These PSD are derived from isotherms shown in Figure 3.

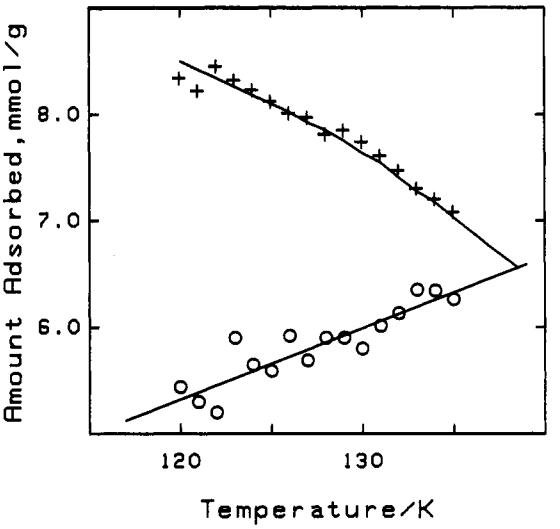

Figure 5. Amount of argon adsorbed on SG3 as capillary liquid (+; desorption branch) and as capillary gas (○; adsorption branch) at the capillary phase transition. The two lines intersect at T_{cc}, and ΔA is their difference at each T.

$$T_{xc} = T_x[1 - (\Delta X)^3] \tag{16}$$

where T_{xc} is the corrected temperature associated with ΔX. The complete set of T_{xc}, ΔX data are analyzed as before (eqs 7–11). Calculations for xenon adsorbed on SG3 are summarized in Table 4, and the PSD obtained for this and other adsorptives are shown in Figure 4. Comparison of ΔA_n, T_n values for xenon on SG3 in Table 1 with corresponding ΔX, T_{xc} values in Table 4 show that the procedures used to calculate T_{xc} (eqs 12–16) give values

that are in reasonable agreement with experiment. Furthermore, PSD derived from a variety of single isotherms are also in reasonable agreement with the more exact corresponding PSD based on a large number of isotherms.

Clearly, for adsorbents with a sufficiently wide range of pore sizes, the smallest pore measurable, at temperature T, will be determined primarily by the properties of the adsorptive, namely, critical temperature (T_c) and diameter (d), through eq 1. For example, the critical pore radius for nitrogen at 77.35 K is 0.99 nm (T_c = 126.26 K, d = 0.383 nm), and pores of smaller radii will not exhibit hysteresis. Therefore, the lower closure point of the hysteresis loop, calculated from the Kelvin equation, eq 14, should occur at relative pressure 0.38. This result is in excellent agreement with the general observation that for nitrogen adsorbed on a wide variety of porous adsorbents at *ca.* 77 K the lower closure point of the hysteresis loop often occurs close to 0.4 relative pressure.[1] This behavior should be characteristic of all adsorptives on suitable adsorbents. For several of the systems listed in Table 3, calculated minimum relative pressures at the lower closure points of the hysteresis loops are in excellent agreement with experimental values.

Conclusions

While the method of pore size analysis requiring numerous isotherms over a wide temperature range is unlikely to become routine, the single isotherm method of analysis can provide a useful description of many rigid, porous adsorbents. When the PSD is known, the arguments used to develop this simplified method may also be used to estimate the complete isotherm for any adsorptive. That is, if an isotherm is known for one adsorptive, then a corresponding isotherm can be calculated for any other adsorptive.

Acknowledgment. Mr. R. Bartholomew measured the adsorption isotherm for *n*-butane on silica gel SG3, Mr. D. Porter measured the tetrachloromethane isotherms, and Mr. B. Kieley measured the oxygen isotherm. Dr. A. J. Brown, Dr. C. G. V. Burgess, and Dr. S. Nuttal generously granted permission to use data from their Ph.D. theses. Professor P. D. Golding provided many useful comments and discussion. This work was supported, in part, by the Natural Sciences and Engineering Research Council of Canada.